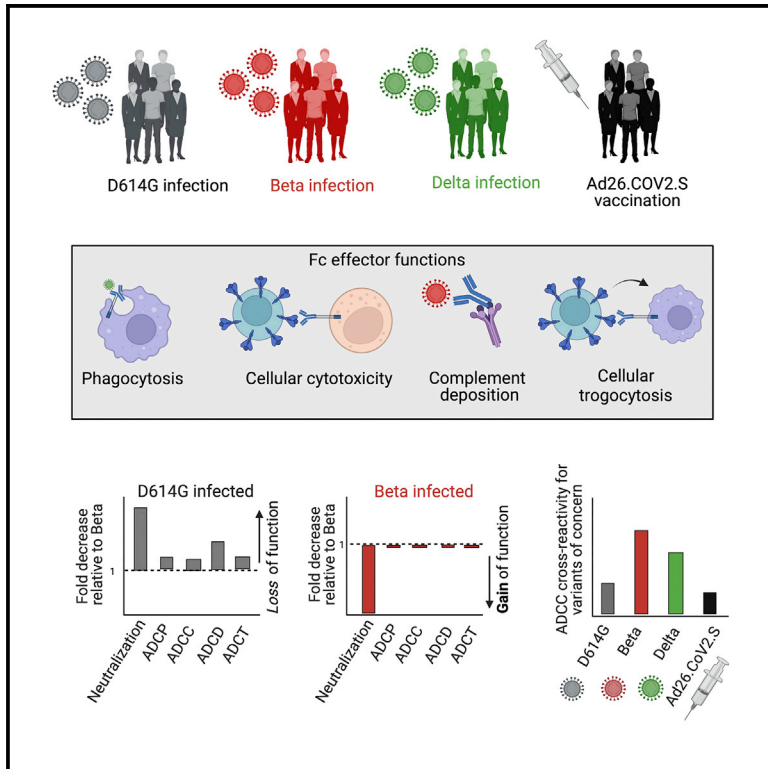# SARS-CoV-2 Beta and Delta variants trigger Fc effector function with increased cross-reactivity

Graphical abstract

Authors

Simone I. Richardson, Nelia P. Manamela, Boitumelo M. Motsoeneng, ..., Ntobeko A.B. Ntusi, Wendy A. Burgers, Penny L. Moore

Correspondence

pennym@nicd.ac.za

In brief

Beyond neutralization, antibodies trigger cytotoxic functions associated with SARS-CoV-2 vaccine protection. Richardson et al. show that these functions are retained against variants of concern (VOC) and that infection by VOCs triggers cross-reactive cytotoxic antibodies. This suggests that SARS-CoV-2 VOC could be used as the basis of vaccines triggering enhanced immune breadth.

Highlights

- Fc effector functions are preserved against SARS-CoV-2 variants of concern (VOCs)

- Complement deposition against VOCs is reduced more than other functions

- VOC infection triggers improved Fc cross-reactivity compared with vaccination

- The sequence of the infecting virus determines the breadth of the Fc response

CellPress

Report

SARS-CoV-2 Beta and Delta variants trigger Fc effector function with increased cross-reactivity

Simone I. Richardson,[1,2] Nelia P. Manamela,[1,2] Boitumelo M. Motsoeneng,[1,2] Haajira Kaldine,[1,2] Frances Ayres,[1,2] Zanele Makhado,[1,2] Mathilda Mennen,[9] Sango Skelem,[9] Noleen Williams,[9] Nancy J. Sullivan,[3] John Misasi,[3] Glenda G. Gray,[4] Linda-Gail Bekker,[5] Veronica Ueckermann,[6] Theresa M. Rossouw,[7] Michael T. Boswell,[6] Ntobeko A.B. Ntusi,[8,9,10,12] Wendy A. Burgers,[8,11,12] and Penny L. Moore[1,2,8,13,14,*]

[1]National Institute for Communicable Diseases of the National Health Laboratory Services, Johannesburg 2131, South Africa
[2]SA MRC Antibody Immunity Research Unit, School of Pathology, University of the Witwatersrand, Johannesburg 2001, South Africa
[3]Vaccine Research Center, National Institute of Allergy and Infectious Diseases, National Institutes of Health, Bethesda, MD 20892, USA
[4]The South African Medical Research Council, Tygerberg 7505, South Africa
[5]The Desmond Tutu HIV Centre, University of Cape Town, Cape Town 7705, South Africa
[6]Division for Infectious Diseases, Department of Internal Medicine, Steve Biko Academic Hospital and University of Pretoria, Pretoria 0002, South Africa
[7]Department of Immunology, Faculty of Health Sciences, University of Pretoria, Pretoria 0028, South Africa
[8]Institute of Infectious Disease and Molecular Medicine, University of Cape Town, Cape Town 7701, South Africa
[9]Cape Heart Institute, Faculty of Health Sciences, University of Cape Town, Cape Town 7701, South Africa
[10]Department of Medicine, University of Cape Town and Groote Schuur Hospital, Cape Town 7701, South Africa
[11]Division of Medical Virology, Department of Pathology, University of Cape Town, Cape Town 7701, South Africa
[12]Wellcome Centre for Infectious Diseases Research in Africa, University of Cape Town, Cape Town 7701, South Africa
[13]Centre for the AIDS Programme of Research in South Africa, Durban 4013, South Africa
[14]Lead contact
*Correspondence: pennym@nicd.ac.za
https://doi.org/10.1016/j.xcrm.2022.100510

SUMMARY

Severe acute respiratory syndrome coronavirus-2 (SARS-CoV-2) variants of concern (VOCs) exhibit escape from neutralizing antibodies, causing concern about vaccine effectiveness. However, while non-neutralizing cytotoxic functions of antibodies are associated with improved disease outcome and vaccine protection, Fc effector function escape from VOCs is poorly defined. Furthermore, whether VOCs trigger Fc functions with altered specificity, as has been reported for neutralization, is unknown. Here, we demonstrate that the Beta VOC partially evades Fc effector activity in individuals infected with the original (D614G) variant. However, not all functions are equivalently affected, suggesting differential targeting by antibodies mediating distinct Fc functions. Furthermore, Beta and Delta infection trigger responses with significantly improved Fc cross-reactivity against global VOCs compared with D614G-infected or Ad26.COV2.S-vaccinated individuals. This suggests that, as for neutralization, the infecting spike sequence affects Fc effector function. These data have important implications for vaccine strategies that incorporate VOCs, suggesting these may induce broader Fc effector responses.

INTRODUCTION

Continued severe acute respiratory syndrome coronavirus-2 (SARS-CoV-2) transmission worldwide through inadequate vaccine coverage has resulted in the emergence of viral variants of concern (VOCs), including Alpha (B.1.1.7), Beta (B.1.351), Gamma (P.1), and Delta (B.1.617.2). These VOCs are able to evade neutralizing responses in vaccinee and convalescent sera,[1–6] although T cell function and spike-binding antibody levels retain activity.[4,7–9] In addition to mediating neutralization, antibodies drive effector functions through their ability to engage cellular receptors via their Fc portion, including antibody-dependent cellular cytotoxicity (ADCC), cellular phagocytosis (ADCP), cellular trogocytosis (ADCT), or cell membrane nibbling and complement deposition (ADCD). Cross-reactive binding antibodies are consistent with pre-

served Fc effector function in convalescent sera and after vaccination, and that several vaccines maintain effectiveness against VOCs.[2,7,10] For example, the Ad26.COV.2S vaccine maintained efficacy against severe coronavirus disease 2019 (COVID-19) illness caused by Beta despite reduced neutralization titers.[2,4,5,11]

Most antibodies elicited by infection are non-neutralizing.[12] As mutations in VOCs occur primarily in the receptor-binding domain (RBD) and the N-terminal domains (NTDs) targeted by neutralizing antibodies, antibodies able to bind outside of these sites and mediate potent antiviral function may confer protection from severe disease. As for other diseases, Fc effector function is associated with reduced COVID-19 severity and mortality, suggesting an important early role for these functions in disease outcome.[13,14] Furthermore, isolated antibodies from convalescent donors require Fc function for optimal protection and therapeutic
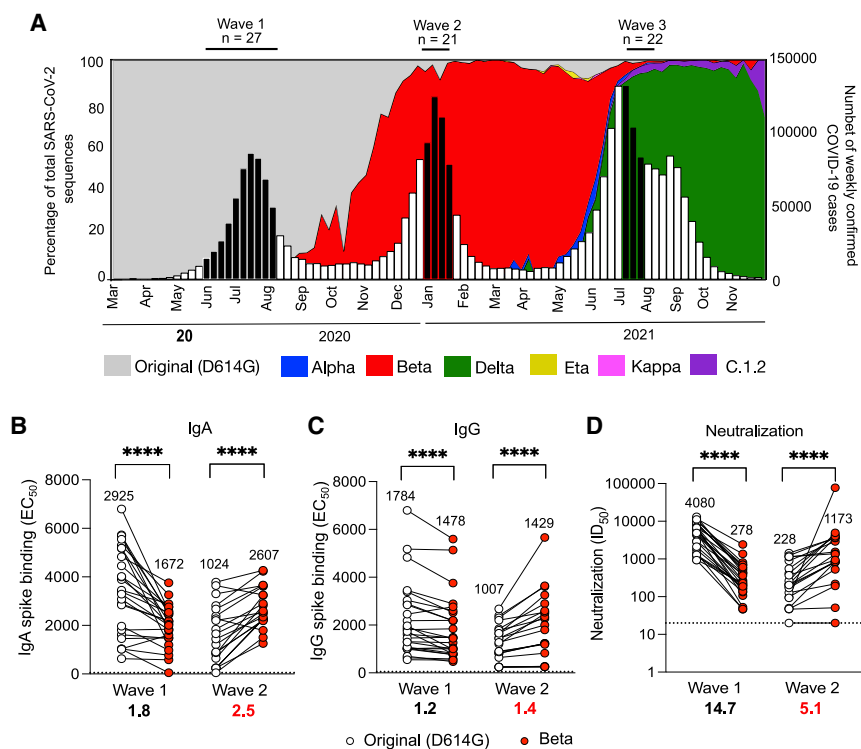
Figure 1. Binding and neutralization of plasma from hospitalized SARS-CoV-2 convalescent individuals sampled in waves driven by distinct viral lineages

(A) The number of SARS-CoV-2 cases in South Africa per epidemiological week from March 2020 to November 2021 (right y axis) is represented by bars, with black bars indicating the period that the wave 1 (n = 27), wave 2 (n = 21), and wave 3 (n = 22) samples were obtained. The percentage of total SARS-CoV-2 sequences over time (left y axis) is shown as a line plot where the proportions of the original D614G, Alpha, Beta, Gamma, Delta, Eta, Kappa, and C.1.2 lineages are shown.

(B and C) (B) IgA and (C) IgG-binding levels by ELISA of wave 1 or wave 2 samples against the original (D614G) (white) or Beta (red) spike.

(D) Neutralization of original (D614G) or Beta pseudoviruses by wave 1 and 2 plasma. Limits of detection are shown with dotted lines, geometric mean titers are shown, and fold change decrease in black and fold change increase in red below the graph. All results are the mean of two independent experiments. Statistical significance between variants was calculated using Wilcoxon paired t test: **p < 0.01; ****p < 0.0001.

efficacy.[15,16] Fc functions persist beyond neutralizing responses following SARS-CoV-2 infection, and may be important for vaccine design.[17,18]

Fc effector function correlated with protection through vaccination in non-human primates[10,19,20] and is elicited by vaccination in humans.[2,7,21,22] Beyond this, nuances in magnitude and breadth of Fc receptor-binding responses from convalescent donors and different vaccine regimens suggest these responses vary by specific antigens, formulations, or doses.[23]

For neutralization, the sequence of the infecting virus affects the breadth of the resulting neutralizing antibodies.[3,9,24] Neutralizing antibodies triggered by VOCs show varying patterns of breadth compared with the original D614G and one another, suggesting that spikes with different genotypes differentially affect the repertoire of triggered antibodies. However, similar studies characterizing Fc effector functions in infections by VOC have not been conducted. Since March 2020, South Africa experienced three distinct waves of COVID-19 infection, each dominated by a different variant. We leveraged these virologically distinct waves to define Fc effector response escape from VOCs, and to describe Fc responses to VOCs. We used convalescent sera from individuals infected with D614G to show that Beta partially evades several Fc effector functions. However, individuals infected with Beta developed Fc effector function with improved cross-reactivity for all VOCs. Lastly, we show that Fc effector function elicited by the Ad26.COV.2.S vaccine is largely retained across VOCs but is not as cross-reactive as those elicited by Beta. Therefore, VOCs differentially trigger Fc effector functions, with implications for vaccination.

RESULTS

Binding antibodies, unlike neutralizing antibodies, retain a high level of activity against heterologous variants

South Africa's first wave peaked in mid-July 2020, the second in January 2021, and the third in August 2021 (Figure 1A). The first wave was dominated by Wuhan D614G, the second by the Beta variant, and the third wave by Delta. We used convalescent plasma from the first two waves (first wave n = 27; second wave n = 21) to determine its ability to bind and neutralize original (D614G) or Beta. First- and second-wave participants were hospitalized patients, matched in age with a median of 52 years (range 27–72 years) and 55 years (range 24–73 years), respectively. Samples were collected a median of 10 days (range 7–33 days) and 13 days (range 2–29 days) after a positive SARS-CoV-2 PCR test (Table S1). Although wave 1 viral sequences were not obtained, these samples were collected several months prior to the emergence of Beta and were assumed to have been D614G infections (Figure 1A). Wave 2 samples were collected when Beta accounted for >90% of infections in the region, with sequences from nasal swabs of all eight samples available from 21 patients confirmed as Beta (Table S1), as described previously.[24]

Comparison of immunoglobulin (Ig) A and IgG binding from wave 1 plasma to the original (D614G) or Beta spikes showed a significant decrease in binding to Beta (Figures 1B and C). In contrast, wave 2 plasma from Beta infections showed a significant increase in both IgA and IgG binding to Beta. However, the differences in geometric mean titer against the original and Beta spike for wave 1 and 2 plasma were less than 2-fold for both IgG and IgA. In
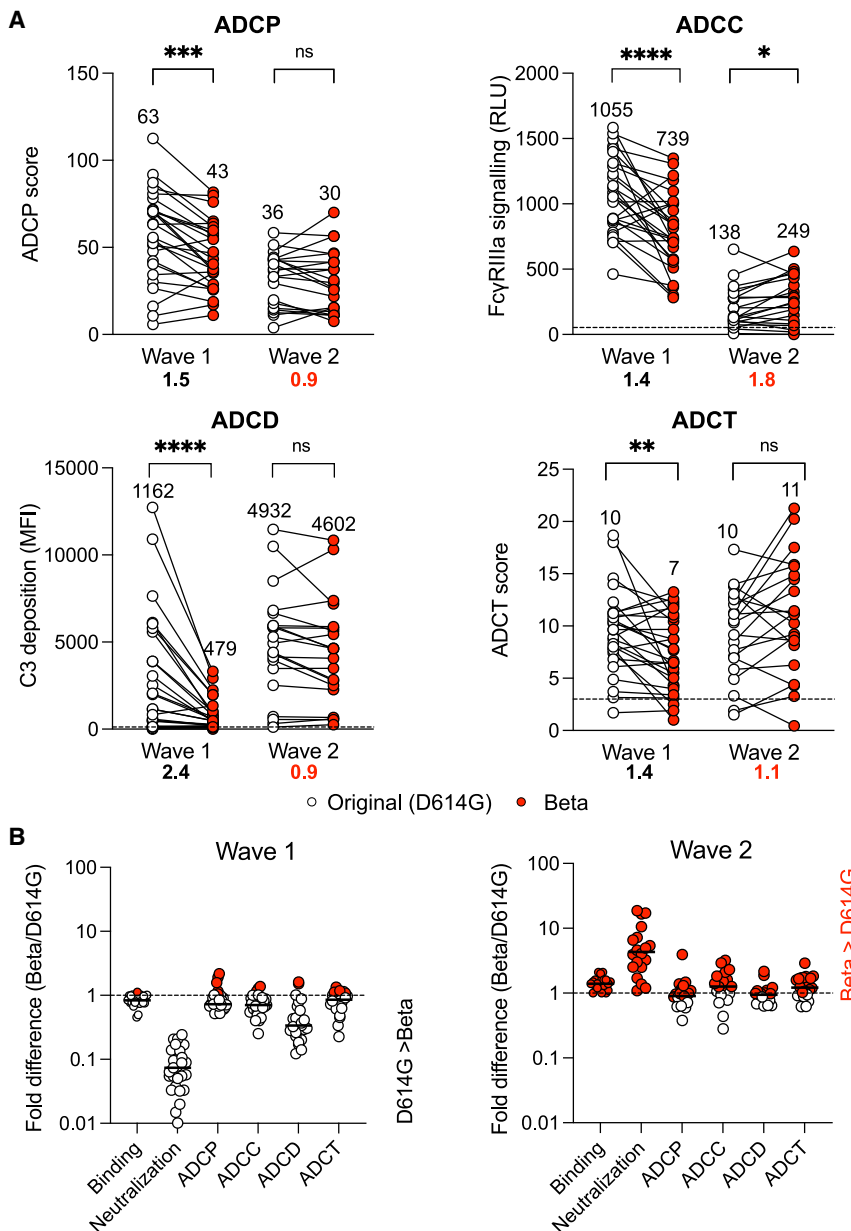
Figure 2. Fc effector function is largely preserved against Beta

(A) Fc effector functions of wave 1 and wave 2 plasma against either original (white) and Beta (red) spike protein or spike-expressing cells. ADCP is represented as the percentage of monocytic cells that take up spike-coated beads multiplied by their geometric mean fluorescence intensity (MFI). ADCC shown as relative light units (RLU) signaling through FcγRIIIa expressing cells. ADCD is shown as the MFI of C3 deposition on spike-coated beads and ADCT represented as the relative proportion of biotinylated spike-expressing cell membrane on carboxyfluorescein succinimidyl ester (CFSE)-positive monocytic cells. Dotted lines indicate the limit of detection and all samples are represented following the subtraction of background. Median values of all functions are shown above the graphs and fold change decrease in black and fold change increase in red below the graph. Results are representative of two independent experiments. Statistical significance between variants is calculated using Wilcoxon paired t test; *p < 0.05; **p < 0.01; ***p < 0.001; ****p < 0.0001; and ns = non-significant.

(B) Fold difference of functions against Beta relative to the original variant for wave 1 and 2 samples where the dotted line indicates no change between variants (red = Beta > D614G; white = D614G < Beta). The median of the fold changes is indicated by lines

contrast, neutralization titers in plasma from wave 1 decreased 14.7-fold against Beta, while wave 2 titers of Beta were 5.1-fold higher than those of D614G (Figure 1C), as we previously showed.[6,24] This difference in reduction of binding versus neutralizing antibodies confirms the ability of convalescent plasma to target epitopes beyond the neutralizing epitopes mutated in VOCs.

Cross-reactivity of Fc effector function is differentially affected by the sequence of the infecting spike

We next measured whether Fc effector functions elicited by the original D614G variant or the Beta variant were equivalent in magnitude and cross-reactivity. We measured spike-specific Fc responses using spike protein coated onto fluorescent beads

(for ADCP and ADCD) or spike expressed on the surface of target cells (ADCC and ADCT). To validate these assays, we tested monoclonal antibodies previously characterized for cell surface spike binding to D614G and Beta.[25] A23–58.1, B1-182.1, A19–46.1, and A19–61.1 have previously been shown to bind D614G and Beta equivalently, and showed similar ADCP, ADCC, ADCD, and ADCT activity against both D614G and Beta (Figure S1). Similarly, class 4 monoclonal antibody (mAb) CR3022, which binds to regions of the RBD that exclude sites mutated in Beta,[26] showed similar Fc effector function for both variants, indicating that these assays were comparable across variants. For class 2 mAbs BD23, LY-CoV555, and P2B-2F6, which are unable to bind or neutralize Beta,[6,27] Fc effector function against Beta was also reduced.

Plasma from wave 1 participants showed a significantly decreased ability to mediate ADCP, ADCC, ADCD, and ADCT of Beta, compared with the original D614G spike, although all retained some activity against Beta (Figure 2A). However, not all Fc effector functions were affected to the same extent. ADCP, ADCC, and ADCT showed 1.5-, 1.4-, and 1.4-fold decreases, similar to the 1.2-fold decrease observed for binding antibodies; however, ADCD showed a 2.4-fold drop (Figures 2A and 2B). This suggests epitope-specific functional responses exist. In
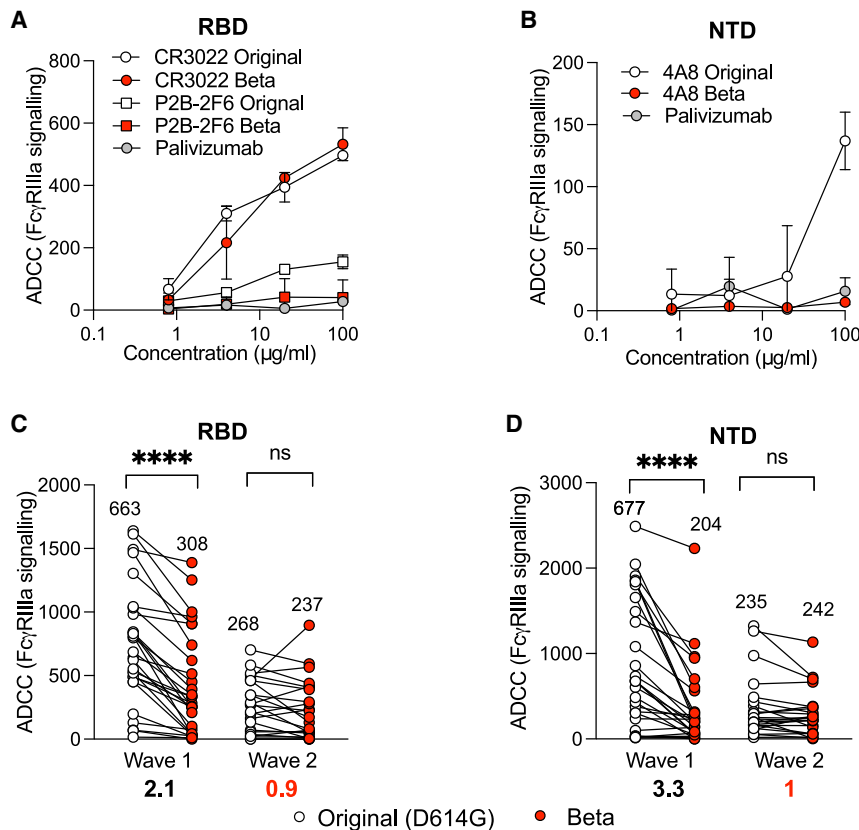
Figure 3. ADCC targets the RBD and NTD and is partially escaped by Beta

(A) ADCC of monoclonal antibodies CR3022, P2B-2FB, and palivizumab shown as RLU of signaling through FcγRIIIa expressing cells and crosslinking of original (white) or Beta (red) (K417N, E484K, and N501Y) RBD protein. Error bars indicate standard deviation of the mean of two independent experiments.

(B) ADCC of monoclonal antibodies 4A8 and palivizumab against original (white) or Beta (red; L18F, D80A, D215G, 242–244 del) NTD protein.

(C and D) Wave 1 and wave 2 plasma against original (white) or Beta (red) (C) RBD or (D) NTD protein. All plots are representative of a minimum of two independent experiments. Median values of all functions are shown above the graphs with fold change decrease in black and fold change increase in red below the graph. Statistical significance between variants was calculated using Wilcoxon paired t test; ****p < 0.0001 and ns = non-significant

nificant difference in IgG-binding titers and ADCT activity to the autologous infecting spike (original or Beta respectively) (Figures 1C and 2A; Figure S2F). However, despite being run in head-to-head assays with wave 1 plasma, the wave 2 plasma showed significantly lower neutralization, ADCP and ADCC activity, and enhanced ability to deposit complement protein compared with wave 1 plasma against autologous spike (Figure S2F). This shows that Fc effector VOC cross-reactivity is not a result of binding titer. Overall, preserved Fc effector function but substantial loss in neutralization against Beta in wave 1 samples (Figure 2B) suggests targeting by Fc effector function is distinct from that of neutralization.

ADCC targets both the NTD and RBD regions of SARS-CoV-2 VOCs

Although Fc effector function elicited by the original D614G virus was not completely abrogated against Beta, the significant decrease in activity suggests that NTD and RBD, mutated in Beta, are substantial targets. Given the significant decrease of ADCC observed against Beta by wave 1 plasma (Figure 2A) we mapped these responses. We determined the contribution to ADCC of antibodies to NTD and RBD by measuring FcγRIIIa signaling as a result of crosslinking to NTD or RBD proteins from the D614G and Beta variants.

We confirmed our ability to map these responses using monoclonal antibodies. As for full spike (Figure S1), CR3022 ADCC against the RBD was unaffected by Beta RBD mutations (K417N, E484K, and N501Y), while ADCC mediated by P2B-2F6 was abrogated (Figure 3A). 4A8, an NTD mAb for which neutralization and binding are escaped by Beta (L18F, D80A, D215G, and 242–244 del),[6] showed ADCC activity against the original variant but not Beta RBD (Figure 3B).

contrast, wave 2 plasma from Beta-infected individuals mediated similar Fc function across the variants tested, with the exception of ADCC (Figure 2A), indicating the elicitation of more cross-reactive responses by this VOC. While wave 2 plasma samples mediated ADCP, ADCD, and ADCT to similar levels against D614G and Beta spikes, ADCC was significantly higher against Beta (Figure 2A) (median D614G ADCC = 138, Beta ADCC = 249, 1.8-fold difference). The other Fc functions tested showed fold differences close to one for wave 2 samples (0.8, 0.9, and 1.1 for ADCP, ADCD, and ADCT respectively) (Figures 2A and 2B).

As Fc effector function is modulated by Fc receptor binding, we examined the ability of antibodies from wave 1 and 2 to crosslink dimeric Fcγ receptors FcγRIIa or FcγRIIIa (which modulate ADCP and ADCC, respectively) and the original or Beta spike protein by ELISA. As expected, Spearman's correlations >0.5 were noted between FcγRIIa binding and ADCP score, and between FcγRIIIa binding and ADCC against original D614G spike (Figures S2A and S2B). Similar to the functional readout, wave 1 samples showed significant decreases in Beta-specific FcγRIIa (Figure S2C) and FcγRIIIa crosslinking (Figure S2D), while no significant differences were noted for wave 2 samples (Figure S2E).
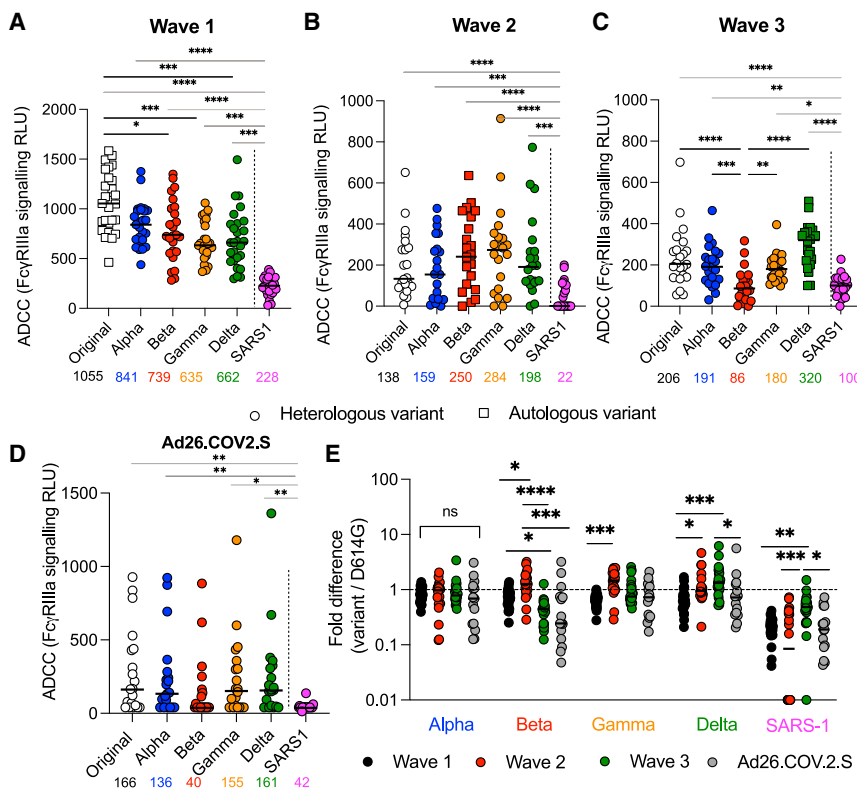
We considered the possibility that differences in Fc effector function simply reflected varying IgG levels between waves, although the samples had been matched for age, severity, and time since PCR test. Wave 1 and wave 2 samples showed no sig-

Figure 4. Beta and Ad26.COV.2.S-elicited ADCC responses are cross-reactive against variants of concern

(A–D) ADCC of (A) wave 1, (B) wave 2, (C) wave 3, (D) Ad26.COV.2.S vaccinee plasma (day 28) against the original, VOC, and SARS-CoV-1 representative of two independent experiments. Bars indicate the median, represented below the graphs with squares indicating the ADCC against the autologous variant and circles indicating ADCC against the heterologous variants. Statistical significance was calculated using the Friedman test, with Dunn's multiple test comparisons, where gray lines indicate significance between SARS-CoV-2 and SARS-CoV-1 and black lines between SARS-CoV-2 variants.

(E) Fold difference represented as ADCC activity against the variant for wave 1, wave 2, wave 3, or vaccine plasma relative to the original. The dotted line represents no fold difference, while lines indicate the median. Statistical differences between waves and vaccine responses were calculated using the Kruskal-Wallis test with Dunn's multiple test comparisons. $*p < 0.05$, $***p < 0.001$, $****p < 0.0001$, and ns = non-significant.

ADCC mediated by wave 1 plasma showed a 2.2-fold decrease against Beta RBD (median 663 and 308 for original and Beta respectively), confirming that, while K417, E484, and N501 sites are targeted, they do not account for the majority of ADCC activity against RBD (Figure 3C). Beta-elicited ADCC did not show significant differences between the original or Beta RBD (Figure 3C), suggesting broader tolerance of RBD mutations in wave 2 plasma, as with neutralization. Similarly, ADCC was detected against the original NTD protein with a 3-fold decrease (median 677 to 204) against Beta in wave 1 plasma (Figure 3C). This may indicate that ADCC antibodies more frequently target NTD sites mutated in Beta (L18, D80, D215), or are less able to tolerate the conformation change of the NTD that may result from the 242–244 deletion. Conversely, as for RBD, ADCC elicited by Beta was not significantly different against the original or Beta NTD (Figure 3C). Therefore, NTD and RBD are targets of ADCC responses in convalescent plasma, but mutations in these regions that confer neutralization escape in original (D614G) infections only slightly affect ADCC.

Beta-elicited ADCC shows greater cross-reactivity against a panel of global VOCs compared with wave 1 infection and Ad26.COV2.S vaccination

As Beta-elicited plasma showed enhanced cross-reactivity for the original variants, we assessed a larger panel of VOCs (D614G and Alpha, Beta, Gamma, Delta, and SARS-1). Samples and VOC were run head to head and normalized by CR3022 ADCC activity.

For wave 1 sera, despite high levels of ADCC against the autologous original variant (median 1,055), ADCC against all heterologous spikes except for Alpha (median 841) was significantly reduced (Beta, 739; Gamma, 635; and Delta, 662) (Figure 4A). The most dramatic reduction in activity was observed against SARS-1 (median, 228). In contrast, wave 2 plasma showed similar ADCC levels for VOCs (Figure 4B), with Gamma-specific ADCC showing the highest level (median 284), followed by Beta, Delta, Alpha, and D614G (250, 198, 159, and 138 respectively). SARS-1 ADCC was significantly lower. Thus, Beta-elicited ADCC activity is cross-reactive for other VOCs, whereas ADCC in response to the original (D614G) variant was substantially less cross-reactive.

To assess whether Delta, which dominated the third wave, also triggered ADCC with increased cross-reactivity, we tested 22 samples from the third wave. Of these, sequences were available from nine, and all were Delta (Table S1). Delta-specific ADCC showed the highest level (median 320), followed by the original, Alpha, and Gamma (median 206, 191, and 180 respectively). However, wave 3 plasma ADCC was significantly reduced against Beta (median 86) (Figure 4C) and SARS-1. Thus, Delta triggers ADCC that is more cross-reactive than the original variant but less cross-reactive than that triggered by Beta.

We next compared ADCC VOC cross-reactivity to infection with the Janssen/Johnson and Johnson Ad26.COV.2.S vaccination. ADCC was measured 28 days post vaccination in 19 individuals confirmed to be SARS-CoV-2 naive.[9] Beta was the most ADCC resistant of the VOCs tested, showing a 3-fold decrease compared with the original variant (median of 40 compared with 166), whereas ADCC against all other variants

showed similar or less than 2-fold decreases (Figure 4D) (fold change relative to the original: Alpha, 1.2; Gamma, 1.1; Delta, 1). Responses to SARS-1 were significantly lower.

Vaccine and wave 1 ADCCs against VOCs were similar, indicating comparable levels of cross-reactivity (Figure 4E). Strikingly, though, vaccine-elicited plasma showed decreased capacity to perform ADCC against Beta compared with wave 1 plasma (Figure 4E). For Beta, Delta, and Gamma, the fold differences for wave 2 sera were consistently >1, and significantly different from wave 1 and Ad26.COV2.S, while Alpha showed no difference (Figure 4E). Wave 3 plasma showed substantially higher reactivity against Delta and SARS-1 than wave 1, wave 2, and Ad26.COV2.S. This further indicates that the sequence of the infecting spike affects the cross-reactivity of Fc responses. Overall, Beta- and Delta-elicited ADCCs showed greater cross-reactivity to global VOCs compared with the original elicited ADCC by either vaccination or infection.

DISCUSSION

Neutralization-resistant variants have compromised vaccine protection from infection, but often not from severe disease. This has highlighted the potential role of other immune functions, including Fc effector functions, in mitigating disease severity. Previous studies have shown sustained activity against VOCs for both convalescent donors and vaccinees.[7,10,23] Here, we confirm overall preservation of Fc effector function against VOCs in infection and vaccination, but show that the magnitude of Fc effector activity against Beta is reduced. Furthermore, escape varies by function, suggesting that antibodies mediating different Fc functions have distinct epitopes. We also assessed Fc function in individuals infected with VOCs. We show that, compared with either the original variant, Delta, or Ad26.COV2.S vaccination, infection with Beta imprints significantly improved Fc cross-reactivity against global VOCs, and that these antibodies target epitopes distinct from those of neutralizing antibodies.

Several studies now support the notion that, unlike neutralization, Fc effector function is more resilient in the face of VOCs.[7,23] Here, we showed preservation of Fc effector function against VOCs both in individuals previously infected with the original D614G variant and in individuals vaccinated with Ad26.COV2.S. This is supported by a recent study measuring natural killer (NK) activation, ADCP, ADCD, and ADCC in Ad26.COV2.S vaccinees showing differences of under 2-fold between original D614G and Beta.[2] Further, this is translatable for NK activation and ADCP across other vaccine modalities, including mRNA-1273 and BNT162b2[7,23]

While Fc effector functions against Beta were only slightly lower, loss of activity was not equivalent for all functions, with ADCD most affected. RBD is a major target for complement binding in both vaccinated and convalescent individuals,[28] which may explain why ADCD has greater loss against Beta, which has RBD mutations. In contrast to ADCD, ADCC activity against Beta was less reduced. Epitope mapping data indicate that Beta RBD and NTD are not the predominant targets of this function. Therefore preservation of ADCC may be the result of antibodies targeting epitopes or sites beyond those commonly mutated in VOCs, such as the S2

region. Differential epitope targeting has also been suggested for other functions, with RBD depletion greatly decreasing antibody-dependent neutrophil phagocytosis (ADNP) activity in contrast to ADCP, which remained unaffected in convalescent plasma.[23] In addition to antibody targeting that varied by function, we also show that individuals infected by different variants have unique Fc effector profiles despite similar levels of binding antibodies. Not all Fc effector functions were affected in the same way; ADCD was higher in wave 2 samples, while ADCC was substantially higher in wave 1. This likely reflects the impact of varying spike sequence on the ability to affect different Fc effector functions, with regions mutated in Beta being dominant targets of ADCD, perhaps as a result of altered steric constraints at the Fc-complement interface. Different VOCs and vaccine platforms may also trigger antibodies with varying glycosylation and/or isotypes.[23,29] These data suggest differential targeting of individual Fc functions in response to VOC, and future studies should include detailed mapping of Fc effector function targets.

We also show subtle differences in the ability of antibodies elicited by either the original D614G or the Ad26.COV2.S vaccine to perform ADCC against Beta. This was despite the fact that the sequence of immunodominant regions of the eliciting immunogens were the same, with only the single D614G mutation differing between them. Similar findings have been reported for ADCP, where RBD is targeted to varying levels in different vaccine modalities and convalescent plasma.[23] This suggests that, beyond sequence, nuanced differences in antigen stability and presentation affect functional responses to vaccination or infection.

We have previously shown that Beta infection imprints a cross-reactive neutralizing response.[3,24] Here we show that this also extends to Fc effector function and other VOCs, including Delta, suggesting that features intrinsic to each spike shape the antibody repertoire. However, the pattern of breadth between neutralization and Fc effector function is not necessarily the same for a given spike. For neutralization, Beta and Delta VOCs are serologically distant, with little cross-neutralization.[30,31] However, for ADCC, cross-reactivity is enhanced against Delta by Beta-elicited plasma, although the converse is not true. This further points to the divergent impact that sequence of immunogen may have on neutralization and Fc effector function.

These data suggest that the spike sequence of the priming immunogen is likely to determine unique Fc effector function profiles, allowing for their potential modulation in future vaccine design. However, this should be considered in the context of neutralization for which the choice of immunogen sequence is far more constrained and alongside which Fc effector function is likely to play a supporting role in protection. While current vaccines provide sufficient protection against severe disease, vaccination strategies may be improved by a spike immunogen associated with a more balanced and broad response.

Limitations of this study

While we have used a national database that tracks PCR confirmation of COVID-19 infection, and our clinical data excluded known cases of prior symptomatic infection, we cannot rule out the possibility of asymptomatic prior infections.

STAR★METHODS

Detailed methods are provided in the online version of this paper and include the following:

- KEY RESOURCES TABLE
- RESOURCE AVAILABILITY
  - Lead contact
  - Materials availability
  - Data and code availability
- EXPERIMENTAL MODEL AND SUBJECT DETAILS
  - Human subjects
- METHOD DETAILS
  - SARS-CoV-2 spike genome sequencing
  - SARS-CoV-2 antigens
  - SARS-CoV-2 spike enzyme-linked immunosorbent assay (ELISA)
  - Spike plasmid and lentiviral pseudovirus production
  - Pseudovirus neutralization assay
  - Antibody-dependent cellular phagocytosis (ADCP) assay
  - Antibody-dependent cellular cytotoxicity (ADCC) assay
  - Antibody-dependent complement deposition (ADCD) assay
  - Antibody-dependent cellular trogocytosis (ADCT) assay
  - Dimeric Fc gamma receptor binding ELISAs
  - Quantification and statistical analysis

SUPPLEMENTAL INFORMATION

Supplemental information can be found online at https://doi.org/10.1016/j.xcrm.2022.100510.

AUTHOR CONTRIBUTIONS

S.I.R. designed the study, performed experiments, analyzed the data, and wrote the manuscript. N.P.M. and B.M.M. performed Fc experiments and analyzed data. H.K. and M.M. performed neutralization assays. F.A. and Z.M. performed ELISA assays. L.G.B. and G.G.G. established the Sisonke Ad26.COV2.S trial. V.U., T.R., and M.B. established the Pretoria COVID-19 study, which provided participant samples from the Steve Biko Academic Hospital. M.M., S.S., and N.W. collected samples and N.A.B.N. and W.A.B. established the Groote Schuur Hospital cohort. N.J.S. and J.M. provided monoclonal antibodies and P.L.M. wrote the manuscript.

REFERENCES

1. Tegally, H., Wilkinson, E., Giovanetti, M., Iranzadeh, A., Fonseca, V., Giandhari, J., Doolabh, D., Pillay, S., San, E.J., Msomi, N., et al. (2021). Detection of a SARS-CoV-2 variant of concern in South Africa. Nature *592*, 438–443. https://doi.org/10.1038/s41586-021-03402-9.

2. Alter, G., Yu, J., Liu, J., Chandrashekar, A., Borducchi, E.N., Tostanoski, L.H., McMahan, K., Jacob-Dolan, C., Martinez, D.R., Chang, A., et al. (2021). Immunogenicity of Ad26.COV2.S vaccine against SARS-CoV-2 variants in humans. Nature. https://doi.org/10.1038/s41586-021-03681-2.

3. Cele, S., Gazy, I., Jackson, L., Hwa, S.-H., Tegally, H., Lustig, G., Giandhari, J., Pillay, S., Wilkinson, E., Naidoo, Y., et al. (2021). Escape of SARS-CoV-2 501Y.V2 from neutralization by convalescent plasma. Nature *593*, 142–146. https://doi.org/10.1038/s41586-021-03471-w.

4. Madhi, S.A., Baillie, V., Cutland, C.L., Voysey, M., Koen, A.L., Fairlie, L., Padayachee, S.D., Dheda, K., Barnabas, S.L., Bhorat, Q.E., et al. (2021). Efficacy of the ChAdOx1 nCoV-19 covid-19 vaccine against the B.1.351 variant. N. Engl. J. Med. https://doi.org/10.1056/NEJMoa2102214.

5. Moore, P.L., Moyo-Gwete, T., Hermanus, T., Kgagudi, P., Ayres, F., Makhado, Z., Sadoff, J., Le Gars, M., van Roey, G., Crowther, C., et al. (2021). Neutralizing antibodies elicited by the Ad26.COV2.S COVID-19 vaccine show reduced activity against 501Y.V2 (B.1.351), despite protection against severe disease by this variant. bioRxiv. http://biorxiv.org/content/early/2021/06/11/2021.06.09.447722.abstract.

6. Wibmer, C.K., Ayres, F., Hermanus, T., Madzivhandila, M., Kgagudi, P., Oosthuysen, B., Lambson, B.E., De Oliveira, T., Vermeulen, M., Van der Berg, K., et al. (2021). SARS-CoV-2 501Y.V2 escapes neutralization by South African COVID-19 donor plasma. Nat. Med. https://doi.org/10.1038/s41591-021-01285-x.

7. Geers, D., Shamier, M.C., Bogers, S., den Hartog, G., Gommers, L., Nieuwkoop, N.N., Schmitz, K.S., Rijsbergen, L.C., van Osch, J.A., Dijkhuizen, E., et al. (2021). SARS-CoV-2 variants of concern partially escape humoral but not T-cell responses in COVID-19 convalescent donors and vaccinees. Sci. Immunol. *6*, eabj1750. http://immunology.sciencemag.org/content/6/59/eabj1750.abstract.

8. Riou, C., Keeton, R., Moyo-Gwete, T., Hermanus, T., Kgagudi, P., Baguma, R., Tegally, H., Doolabh, D., Iranzadeh, A., Tyers, L., et al. (2021). Loss of recognition of SARS-CoV-2 B.1.351 variant spike epitopes but overall preservation of T cell immunity. medRxiv. http://medrxiv.org/content/early/2021/06/06/2021.06.03.21258307.abstract.

9. Keeton, R., Richardson, S.I., Moyo-Gwete, T., Hermanus, T., Tincho, M.B., Benede, N., Manamela, N.P., Baguma, R., Makhado, Z., Ngomti, A., et al. (2021). Prior infection with SARS-CoV-2 boosts and broadens Ad26.COV2.S immunogenicity in a variant dependent manner. medRxiv. http://medrxiv.org/content/early/2021/07/28/2021.07.24.21261037.abstract.

10. Gorman, M.J., Patel, N., Guebre-Xabier, M., Zhu, A.L., Atyeo, C., Pullen, K.M., Loos, C., Goez-Gazi, Y., Carrion, R., Tian, J.H., et al. (2021). Fab and Fc contribute to maximal protection against SARS-CoV-2 following NVX-CoV2373 subunit vaccine with Matrix-M vaccination. Cell Rep. Med. *2*, 100405. https://www.ncbi.nlm.nih.gov/pmc/articles/PMC7899467/.

11. Sadoff, J., Gray, G., Vandebosch, A., Cárdenas, V., Shukarev, G., Grinsztejn, B., Goepfert, P.A., Truyers, C., Fennema, H., Spiessens, B., et al. (2021). Safety and efficacy of single-dose Ad26.COV2.S vaccine against covid-19. N. Engl. J. Med. *384*, 2187–2201. https://doi.org/10.1056/NEJMoa2101544.

12. Amanat, F., Thapa, M., Lei, T., Ahmed, S.M.S., Adelsberg, D.C., Carreño, J.M., Strohmeier, S., Schmitz, A.J., Zafar, S., Zhou, J.Q., et al. (2021). SARS-CoV-2 mRNA vaccination induces functionally diverse antibodies to NTD, RBD, and S2. Cell *184*, 3936–3948.e10. https://www.sciencedirect.com/science/article/pii/S0092867421007066.

13. Richardson, S.I., and Moore, P.L. (2021). Targeting Fc effector function in vaccine design. Expert Opin. Ther. Targets *25*, 467–477. https://doi.org/10.1080/14728222.2021.1907343.

14. Zohar, T., Loos, C., Fischinger, S., Atyeo, C., Wang, C., Slein, M.D., Burke, J., Yu, J., Feldman, J., Hauser, B.M., et al. (2020). Compromised humoral functional evolution tracks with SARS-CoV-2 mortality. Cell *183*, 1508–1519.e12. https://doi.org/10.1016/j.cell.2020.10.052.

15. Schäfer, A., Muecksch, F., Lorenzi, J.C.C., Leist, S.R., Cipolla, M., Bournazos, S., Schmidt, F., Maison, R.M., Gazumyan, A., Martinez, D.R., et al. (2021). Antibody potency, effector function, and combinations in protection and therapy for SARS-CoV-2 infection in vivo. J. Exp. Med. *218*, e20201993. https://rupress.org/jem/article/doi/10.1084/jem.20201993/211549/Antibody-potency-effector-function-and.

16. Winkler, E.S., Gilchuk, P., Yu, J., Bailey, A.L., Chen, R.E., Chong, Z., Zost, S.J., Jang, H., Huang, Y., Allen, J.D., et al. (2021). Human neutralizing antibodies against SARS-CoV-2 require intact Fc effector functions for optimal therapeutic protection. Cell *184*, 1804–1820.e16. http://biorxiv.org/cgi/content/short/2020.12.28.424554v1?rss=1&utm_source=researcher_app&utm_medium=referral&utm_campaign=RESR_MRKT_Researcher_inbound.

17. Anand, S.P., Prévost, J., Nayrac, M., Beaudoin-Bussières, G., Benlarbi, M., Gasser, R., Brassard, N., Laumaea, A., Gong, S.Y., Bourassa, C., et al. (2021). Longitudinal analysis of humoral immunity against SARS-CoV-2 spike in convalescent individuals up to eight months post-symptom onset. Cell Rep. Med. *2*, 100290. https://pubmed.ncbi.nlm.nih.gov/33969322.

18. Lee, W.S., Selva, K.J., Davis, S.K., Wines, B.D., Reynaldi, A., Esterbauer, R., Kelly, H.G., Haycroft, E.R., Tan, H.X., Juno, J.A., et al. (2021). Decay of Fc-dependent antibody functions after mild to moderate COVID-19. Cell Rep. Med. *2*, 100296. https://www.sciencedirect.com/science/article/pii/S2666379121001294.

19. Mercado, N.B., Zahn, R., Wegmann, F., Loos, C., Chandrashekar, A., Yu, J., Liu, J., Peter, L., McMahan, K., Tostanoski, L.H., et al. (2020). Single-shot Ad26 vaccine protects against SARS-CoV-2 in rhesus macaques. Nature *586*, 583–588. http://www.nature.com/articles/s41586-020-2607-z.

20. Yu, J., Tostanoski, L.H., Peter, L., Mercado, N.B., McMahan, K., Mahrokhian, S.H., Nkolola, J.P., Liu, J., Li, Z., Chandrashekar, A., et al. (2020). DNA vaccine protection against SARS-CoV-2 in rhesus macaques. Science *369*, 806–811. http://science.sciencemag.org/cgi/content/short/369/6505/806?rss=1&utm_source=researcher_app&utm_medium=referral&utm_campaign=RESR_MRKT_Researcher_inbound.

21. Barrett, J.R., Belij-Rammerstorfer, S., Dold, C., Ewer, K.J., Folegatti, P.M., Gilbride, C., Halkerston, R., Hill, J., Jenkin, D., Stockdale, L., et al. (2021). Phase 1/2 trial of SARS-CoV-2 vaccine ChAdOx1 nCoV-19 with a booster dose induces multifunctional antibody responses. Nat. Med. *27*, 279–288. http://www.nature.com/articles/s41591-020-01179-4.

22. Tauzin, A., Nayrac, M., Benlarbi, M., Gong, S.Y., Gasser, R., Beaudoin-Bussières, G., Brassard, N., Laumaea, A., Vézina, D., Prévost, J., et al. (2021). A single dose of the SARS-CoV-2 vaccine BNT162b2 elicits Fc-mediated antibody effector functions and T cell responses. Cell Host Microbe *29*, 1137–1150.e6. https://www.sciencedirect.com/science/article/pii/S1931312821002791.

23. Kaplonek, P., Cizmeci, D., Fischinger, S., Collier, A.-R., Suscovich, T., Linde, C., Broge, T., Mann, C., Amanat, F., Dayal, D., et al. (2021). Subtle immunological differences in mRNA-1273 and BNT162b2 COVID-19 vaccine induced Fc-functional profiles. BioRxiv. https://pubmed.ncbi.nlm.nih.gov/34494026.

24. Moyo-Gwete, T., Madzivhandila, M., Makhado, Z., Ayres, F., Mhlanga, D., Oosthuysen, B., Lambson, B.E., Kgagudi, P., Tegally, H., Iranzadeh, A., et al. (2021). Cross-reactive neutralizing antibody responses elicited by SARS-CoV-2 501Y.V2 (B.1.351). N. Engl. J. Med. *384*, 2161–2163. https://doi.org/10.1056/NEJMc2104192.

25. Wang, L., Zhou, T., Zhang, Y., Yang, E.S., Schramm, C.A., Shi, W., Pegu, A., Oloniniyi, O.K., Henry, A.R., Darko, S., et al. (2021). Ultrapotent antibodies diverse and highly transmissible SARS-CoV-2 variants. Science *373*, eabh1766. http://science.sciencemag.org/content/early/2021/06/30/science.abh1766.abstract.

26. Yuan, M., Wu, N.C., Zhu, X., Lee, C.-C.D., So, R.T.Y., Lv, H., Mok, C.K.P., and Wilson, I.A. (2020). A highly conserved cryptic epitope in the receptor binding domains of SARS-CoV-2 and SARS-CoV. Science *368*, 630–633. http://science.sciencemag.org/cgi/content/short/368/6491/630?rss=1&utm_source=researcher_app&utm_medium=referral&utm_campaign=RESR_MRKT_Researcher_inbound.

27. Starr, T.N., Greaney, A.J., Dingens, A.S., and Bloom, J.D. (2021). Complete map of SARS-CoV-2 RBD mutations that escape the monoclonal antibody LY-CoV555 and its cocktail with LY-CoV016. Cell Rep. Med. *2*, 100255. https://www.sciencedirect.com/science/article/pii/S2666379121000719.

28. Klingler, J., Lambert, G.S., Itri, V., Liu, S., Bandres, J.C., Enyindah-Asonye, G., Liu, X., Oguntuyo, K.Y., Amanat, F., Lee, B., et al. (2021). SARS-CoV-2 mRNA vaccines induce a greater array of spike-specific antibody isotypes with more potent complement binding capacity than natural infection. medRxiv. http://medrxiv.org/content/early/2021/05/17/2021.05.11.21256972.abstract.

29. Farkash, I., Feferman, T., Cohen-Saban, N., Avraham, Y., Morgenstern, D., Mayuni, G., Barth, N., Lustig, Y., Miller, L., Shouval, D.S., et al. (2021). Anti-SARS-CoV-2 antibodies elicited by COVID-19 mRNA vaccine exhibit a unique glycosylation pattern. Cell Rep. *37*, 110114. https://www.sciencedirect.com/science/article/pii/S2211124721016089.

30. Cele, S., Karim, F., Lustig, G., James, S.E., Hermanus, T., Wilkinson, E., Snyman, J., Bernstein, M., Khan, K., Hwa, S.H., et al. (2021). Divergence of delta and beta variants and SARS-CoV-2 evolved in prolonged infection into distinct serological phenotypes. medRxiv. http://medrxiv.org/content/early/2021/09/23/2021.09.14.21263564.abstract.

31. Scheepers, C., Everatt, J., Amoako, D.G., Tegally, H., Wibmer, C.K., Mnguni, A., Ismail, A., Mahlangu, B., Lambson, B., Richardson, S., et al. (2021). Emergence and phenotypic characterization of C.1.2, a globally detected lineage that rapidly accumulated mutations of concern. medRxiv. http://medrxiv.org/content/early/2021/09/24/2021.08.20.21262342.abstract.

32. Hadfield, J., Megill, C., Bell, S.M., Huddleston, J., Potter, B., Callender, C., Sagulenko, P., Bedford, T., and Neher, R.A. (2018). Nextstrain: real-time tracking of pathogen evolution. Bioinformatics *34*, 4121–4123. https://doi.org/10.1093/bioinformatics/bty407.

33. Ackerman, M.E., Moldt, B., Wyatt, R.T., Dugast, A.-S., McAndrew, E., Tsoukas, S., Jost, S., Berger, C.T., Sciaranghella, G., Liu, Q., et al. (2011). A robust, high-throughput assay to determine the phagocytic activity of clinical antibody samples. J. Immunol. Methods *366*, 8–19. https://linkinghub.elsevier.com/retrieve/pii/S0022175910003935.

34. Fischinger, S., Fallon, J.K., Michell, A.R., Broge, T., Suscovich, T.J., Streeck, H., and Alter, G. (2019). A high-throughput, bead-based, antigen-specific assay to assess the ability of antibodies to induce complement activation. J. Immunol. Methods *473*, 112630. https://doi.org/10.1016/j.jim.2019.07.002.

35. Richardson, S.I., Crowther, C., Mkhize, N.N., and Morris, L. (2018). Measuring the ability of HIV-specific antibodies to mediate trogocytosis. J. Immunol. Methods *463*, 71–83. https://linkinghub.elsevier.com/retrieve/pii/S0022175918301650.

36. Wines, B.D., Vanderven, H.A., Esparon, S.E., Kristensen, A.B., Kent, S.J., and Hogarth, P.M. (2016). Dimeric FcγR ectodomains as probes of the Fc receptor function of anti-influenza virus IgG. J. Immunol. *197*, 1507–1516.

STAR★METHODS

KEY RESOURCES TABLE

REAGENT or RESOURCE	SOURCE	IDENTIFIER
Antibodies		
CR3022	Genscript (https://www.genscript.com)	N/A
BD23	Dr Nicole Doria-Rose, VRC, USA	N/A
P2B-2F6	Dr Nicole Doria-Rose, VRC, USA	N/A
anti-IgG APC (clone QA19A42)	Biolegend	Cat#366905 RRID:AB_2888847
Palivizumab	Medimmune	Synagis; RRID: AB_2459638
A23-58.1, B1-182.1, A19-46.1 and A19-61.1	John Misasi, VRC, USA	N/A
Bacterial and virus strains		
SARS-CoV-2 pseudoviruses for ancestral, Beta	Wibmer et al., 2021; This paper	N/A
Biological samples		
Convalescent hospitalized blood samples	Groote Schuur Hospital	https://www.gsh.co.za
Convalescent hospitalized blood samples	Steve Biko Academic Hospital	https://www.sbah.org.za
AD26.COV2.S vaccinee blood samples	National institute for Communicable Diseases	https://www.nicd.ac.za
Chemicals, peptides, and recombinant proteins		
SARS-CoV-2 original and Beta variant spike proteins	Original: Dr Jason McKellan Beta: Moyo-Gwete et al., 2021	N/A
Critical commercial assays		
PEI-MAX 40,000	Polysciences	Cat # 24765-1
QUANTI-Luc luciferase	Invivogen	Cat# rep-qlc2
EZ link Sulfo-NHS-LC-Biotin kit	ThermoFisher	Cat# 21435
FluoSpheres™ NeutrAvidin™-Labeled Microspheres, 1.0 μm	ThermoFisher	Cat# F8775 and F8776
Anti-guinea pig complement C3 goat IgG fraction, fluorescein-conjugated	MPBio	Cat# 0855385
Carboxyfluorescein succinimidyl ester (CFSE)	Sigma	Cat# 21888
Luciferase	Promega	Cat# PRE263B-C
Experimental models: Cell lines		
Human Embryonic Kidney (HEK) 293F	Dr Nicole Doria-Rose, VRC, USA	N/A
HEK293T/ACE2.MF	Dr Michael Farzan, Scripps, USA	N/A
Jurkat-Lucia™ NFAT-CD16 cells	Invivogen	Cat # jktl-nfat-cd16
Human Embryonic Kidney (HEK) 293T cells	Dr George Shaw, UPenn,USA	N/A
THP-1 Cells	NIH HIV Reagent program	Cat # ARP-9942
Recombinant DNA		
Spike Hexapro plasmid	Original: Dr Jason McKellan Beta: Moyo-Gwete et al., 2021	N/A
SARS-CoV-2 ancestral variant spike (D614G) plasmid	Wibmer et al., 2021	N/A
Beta spike (L18F, D80A, D215G, K417N, E484K, N501Y, D614G, A701V, 242-244 del) plasmid	Wibmer et al., 2021	N/A

Continued

REAGENT or RESOURCE	SOURCE	IDENTIFIER
Delta spike (T19R, R158G L452R, T478K, D614G, P681R, D950N, 156-157 del) plasmid	Keeton et al., 2021	N/A
Gamma spike (L18F, T20N, P26S, D138Y, R190S, K417T, E484K, N501Y, D614G, H655Y, T1027I, V1176F)	This paper	N/A
Alpha spike (DEL69-70, DEL144, N501Y, A570D, D614G, P681H, T716I, S982A, D1118H)	This paper	N/A
SARS-1	This paper	N/A
Firefly luciferase encoding lentivirus backbone plasmid	Dr Michael Farzan, Scripps	N/A
Software and algorithms		
Genome Detective 1.132	Genome Detective	https://www.genomedetective.com
Coronavirus Typing Tool	Cleemput et al., 2020	N/A
Geneious software	Biomatters Ltd	N/A
NextStrain	Hadfield et al., 2018	https://github.com/nextstrain/ncov
FACSDiva 9	BD Biosciences	https://www.bdbiosciences.com
FlowJo 10	FlowJo, LLC	https://www.flowjo.com
Graphpad Prism 9	Graphpad	https://www.graphpad.com
Biorender	Biorender	https://www.biorender.com

RESOURCE AVAILABILITY

Lead contact
Further information and reasonable requests for resources and reagents should be directed to and will be fulfilled by the lead contact, Penny Moore (pennym@nicd.ac.za).

Materials availability
Materials will be made by request to Penny Moore (pennym@nicd.ac.za).

Data and code availability

- All data reported in this paper will be shared by the lead contact upon request.
- This paper does not report original code.
- Any additional information required to reanalyze the data reported in this paper is available from the lead contact upon request.

EXPERIMENTAL MODEL AND SUBJECT DETAILS

Human subjects
First wave plasma samples (n = 27) were collected from participants enrolled to the Pretoria COVID-19 study cohort. Participants were admitted to Steve Biko Academic Hospital (Pretoria, South Africa) with moderate to severe (WHO scale 4-6) PCR confirmed SARS-CoV-2 infection between May and September 2020 (Figure 1A; Table S1). Ethics approval was received from the University of Pretoria, Human Research Ethics Committee (Medical) (247/2020). Second wave plasma samples were obtained from hospitalized COVID-19 patients (n = 21) with moderate disease (WHO scale 4–5) admitted to Groote Schuur Hospital cohort, Cape Town from December 2020 – January 2021 (Figure 1A; Table S1). This study received ethics approval from the Human Research Ethics Committee of the Faculty of Health Sciences, University of Cape Town (R021/2020). Wave 3 samples (n = 22) were collected from hospitalized COVID-19 patients with moderate disease (WHO scale 4–5) from Steve Biko Academic Hospital and Groote Schuur Hospital in July 2021 (Figure 1A, Table S1) under the aforementioned protocols. All patients had PCR confirmed SARS-CoV-2 infection before blood collection. For the Ad26.COV.2 vaccine samples (n = 19), health care workers were recruited between July 2020 and January 2021 from Groote Schuur Hospital and vaccinated with single dose Johnson and Johnson Ad26.COV2.S in the Sisonke Phase 3b trial between 12 February and 26 March 2021. Lack of prior infection in these individuals was confirmed by Nucleocapsid ELISA as

described.[9] The study was approved by the University of Cape Town Human Research Ethics Committee (HREC 190/2020 and 209/2020) and the University of the Witwatersrand Human Research Ethics Committee (Medical) (no M210429). Written informed consent was obtained from all participants.

Cell lines

Human embryo kidney HEK293T cells were cultured at 37 °C, 5% CO2, in DMEM containing 10% heat-inactivated fetal bovine serum (Gibco BRL Life Technologies) and supplemented with 50 μg/mL gentamicin (Sigma). Cells were disrupted at confluence with 0.25% trypsin in 1 mM EDTA (Sigma) every 48–72 hours. HEK293T/ACE2.MF cells were maintained in the same way as HEK293T cells but were supplemented with 3 μg/mL puromycin for selection of stably transduced cells. HEK293F suspension cells were cultured in 293 Freestyle media (Gibco BRL Life Technologies) and cultured in a shaking incubator at 37 °C, 5% CO2, 70% humidity at 125rpm maintained between 0.2 and 0.5 million cells/mL. Jurkat-Lucia NFAT-CD16 cells were maintained in IMDM media with 10% heat-inactivated fetal bovine serum (Gibco, Gaithersburg, MD), 1% Penicillin Streptomycin (Gibco, Gaithersburg, MD) and 10 μg/mL of Blasticidin and 100 μg/mL of Zeocin was added to the growth medium every other passage. THP-1 cells were used for both the ADCP and ADCT assays and obtained from the AIDS Reagent Program, Division of AIDS, NIAID, NIH contributed by Dr. Li Wu and Vineet N. KewalRamani. Cells were cultured at 37 °C, 5% CO2 in RPMI containing 10% heat-inactivated fetal bovine serum (Gibco, Gaithersburg, MD) with 1% Penicillin Streptomycin (Gibco, Gaithersburg, MD) and 2-mercaptoethanol to a final concentration of 0.05 mM and not allowed to exceed 4×10^5 cells/mL to prevent differentiation.

METHOD DETAILS

SARS-CoV-2 spike genome sequencing

For wave 2 and 3 samples, sequencing of the spike was performed as previously described[24] using swabs obtained from randomly collected Groote Schuur Hospital patients of which eight were included and confirmed as Beta for wave 2 and 9 were included and confirmed as Delta for wave 3 in this study (Table S1). RNA sequencing was performed as previously published.[1] Briefly, extracted RNA was used to synthesize cDNA using the Superscript IV First Strand synthesis system (Life Technologies, Carlsbad, CA) and random hexamer primers. SARS-CoV-2 whole genome amplification was performed by multiplex PCR using primers designed on Primal Scheme (http://primal.zibraproject.org/) to generate 400 bp amplicons with a 70 bp overlap covering the SARS-CoV-2 genome. Phylogenetic clade classification of the genomes in this study consisted of analyzing them against a global reference dataset using a custom pipeline based on a local version of NextStrain (https://github.com/nextstrain/ncov).[32]

SARS-CoV-2 antigens

For ELISA, ADCP and ADCD assays, SARS-CoV-2 original and Beta variant full spike (L18F, D80A, D215G, K417N, E484K, N501Y, D614G, A701V, 242–244 del), RBD original and Beta (K417N, E484K and N501Y, D614G) and NTD original and Beta (L18F, D80A, D215G and 242–244 del) proteins were expressed in Human Embryonic Kidney (HEK) 293F suspension cells by transfecting the cells with the respective expression plasmid. After incubating for six days at 37°C, 70% humidity and 10% CO₂, proteins were first purified using a nickel resin followed by size-exclusion chromatography. Relevant fractions were collected and frozen at −80°C until use.

SARS-CoV-2 spike enzyme-linked immunosorbent assay (ELISA)

Two μg/mL of spike protein (Original or Beta) was used to coat 96-well, high-binding plates and incubated overnight at 4°C. The plates were incubated in a blocking buffer consisting of 5% skimmed milk powder, 0.05% Tween 20, 1× PBS. Plasma samples were diluted to 1:100 starting dilution in a blocking buffer and added to the plates. IgG or IgA secondary antibody was diluted to 1:3000 or 1:1000 respectively in blocking buffer and added to the plates followed by TMB substrate (Thermofisher Scientific). Upon stopping the reaction with 1 M H_2SO_4, absorbance was measured at a 450nm wavelength. In all instances, mAbs CR3022 and BD23 were used as positive controls and Palivizumab was used as a negative control.

Spike plasmid and lentiviral pseudovirus production

The SARS-CoV-2 Wuhan-1 spike, cloned into pCDNA3.1 was mutated using the QuikChange Lightning Site-Directed Mutagenesis kit (Agilent Technologies) and NEBuilder HiFi DNA Assembly Master Mix (NEB) to include D614G (original) or lineage defining mutations for Alpha (DEL69-70, DEL144, N501Y, A570D, D614G, P681H, T716I, S982A, D1118H), Beta (L18F, D80A, D215G, 242-244del, K417N, E484K, N501Y, D614G and A701V), Gamma (L18F, T20N, P26S, D138Y, R190S, K417T, E484K, N501Y, D614G, H655Y, T1027I, V1176F) or Delta (T19R, 156-157del, R158G, L452R, T478K, D614G, P681R and D950N). SARS-1 spike was also cloned into pcDNA.

Pseudotyped lentiviruses were prepared by co-transfecting HEK293T cell line with either the SARS-CoV-2 ancestral variant spike (D614G) or the Beta spike plasmids in conjunction with a firefly luciferase encoding lentivirus backbone plasmid as previously described.[24] Briefly, pseudoviruses were produced by co-transfection in 293T/17 cells with a lentiviral backbone (HIV-1 pNL4.luc encoding the firefly luciferase gene) and either of the SARS-CoV-2 spike plasmids with PEIMAX (Polysciences). Culture supernatants were clarified of cells by a 0.45-μM filter and stored at −70°C. Other pcDNA plasmids were used for the ADCC assay.

Pseudovirus neutralization assay

For the neutralization assay, plasma samples were heat-inactivated and clarified by centrifugation. Heat-inactivated plasma samples from vaccine recipients were incubated with the SARS-CoV-2 pseudotyped virus for 1 hour at 37 °C, 5% CO2. Subsequently, 1×10^4 HEK293T cells engineered to over-express ACE-2 (293T/ACE2.MF)(kindly provided by M. Farzan (Scripps Research)) were added and incubated at 37 °C, 5% CO$_2$ for 72 hours upon which the luminescence of the luciferase gene was measured. Titers were calculated as the reciprocal plasma dilution (ID50) causing 50% reduction of relative light units. CB6 and CA1 was used as a positive control.

Antibody-dependent cellular phagocytosis (ADCP) assay

SARS-CoV-2 original or Beta spike was biotinylated using EZ link Sulfo-NHS-LC-Biotin kit (ThermoFisher) and coated on to fluorescent neutravidin beads as previously described.[33] Briefly, beads were incubated for two hours with monoclonal antibodies at a starting concentration of 2 µg/mL and titrated five-fold or plasma at a single 1 in 100 dilution. Opsonized beads were incubated with the monocytic THP-1 cell line overnight, fixed and interrogated on the FACSAria II. Phagocytosis score was calculated as the percentage of THP-1 cells that engulfed fluorescent beads multiplied by the geometric mean fluorescence intensity of the population less the no antibody control. For this and all subsequent Fc effector assays, pooled plasma from 5 PCR-confirmed SARS-CoV-2 infected individuals and CR3022 were used as positive controls and plasma from 5 pre-pandemic healthy controls and Palivizumab were used as negative controls. In addition samples both waves were run head-to-head in the same experiment. ADCP scores for original and Beta spikes were normalised to each other and between runs using CR3022.

Antibody-dependent cellular cytotoxicity (ADCC) assay

The ability of plasma antibodies to cross-link and signal through FcγRIIIa (CD16) and spike expressing cells or SARS-CoV-2 protein was measured as a proxy for ADCC. For spike assays, HEK293T cells were transfected with 5µg of SARS-CoV-2 original variant spike (D614G), Beta, Gamma, Delta or SARS-1 spike plasmids using PEI-MAX 40,000 (Polysciences) and incubated for 2 days at 37 °C. Expression of spike was confirmed by differential binding of CR3022 and P2B-2F6 and their detection by anti-IgG APC staining measured by flow cytometry. For original or Beta NTD or RBD assays protein was coated at 1 µg/mL on a high binding ELISA 96-well plate and incubated at 4 °C overnight. Plates were then washed with PBS and blocked at room temperature for 1 hr with PBS + 2.5% BSA. Subsequently, protein or 1×10^5 spike transfected cells per well were incubated with heat inactivated plasma (1:100 final dilution) or monoclonal antibodies (final concentration of 100 µg/mL) in RPMI 1640 media supplemented with 10% FBS 1% Pen/Strep (Gibco, Gaithersburg, MD) for 1 hour at 37 °C. Jurkat-Lucia NFAT-CD16 cells (Invivogen) (2×10^5 cells/well and 1×10^5 cells/well for spike and other protein respectively) were added and incubated for 24 hours at 37 °C, 5% CO$_2$. Twenty µL of supernatant was then transferred to a white 96-well plate with 50 µL of reconstituted QUANTI-Luc secreted luciferase and read immediately on a Victor 3 luminometer with 1s integration time. Relative light units (RLU) of a no antibody control was subtracted as background. Palivizumab was used as a negative control, while CR3022 was used as a positive control, and P2B-2F6 to differentiate the Beta from the D614G variant. To induce the transgene 1× cell stimulation cocktail (Thermofisher Scientific, Oslo, Norway) and 2 µg/mL ionomycin in R10 was added as a positive control to confirm sufficient expression of the Fc receptor. CR3022 (for spike and RBD) or 4A8 (NTD) were used as positive controls and Palivizumab were used as negative controls. RLUs for original and Beta spikes were normalised to each other and between runs using CR3022. A cut off of 40 was determined by screening of 40 SARS-CoV-2 naive and unvaccinated individuals. All samples were run head to head in the same experiment as were all variants tested.

Antibody-dependent complement deposition (ADCD) assay

ADCD was measured as previously described.[34] Biotinylated spike protein was coated 1:1 onto red fluorescent 1 µM neutravidin beads (Molecular Probes Inc.) for 2 hours at 37 °C. These were incubated with a single 1:10 plasma sample dilution or 5-fold titration of mAb at a starting concentration of 100 µg/mL for 2 hours and guinea pig complement diluted 1 in 50 with gelatin/veronal buffer for 15 minutes at 37 °C. Beads were washed in PBS and stained with anti-guinea pig C3b-FITC, fixed and interrogated on a FACS Aria II. Complement deposition score was calculated as the percentage of C3b-FITC positive beads multiplied by the geometric mean fluorescent intensity of FITC in this population less the no antibody or heat inactivated controls. ADCD scores for original and Beta spikes were normalised to each other and between runs using CR3022. Both wave 1 and wave 2 samples were run head to head using the same batch of bead preparation.

Antibody-dependent cellular trogocytosis (ADCT) assay

ADCT was performed as described in and modified from a previously described study.[35] HEK293T cells transfected with a SARS-CoV-2 spike pcDNA vector as above were surface biotinylated with EZ-Link Sulfo-NHS-LC-Biotin as recommended by the manufacturer. Fifty-thousand cells per well were incubated with 5-fold titration of mAb starting at 25 µg/mL or single 1 in 100 dilution for 30 minutes. Following a RPMI media wash, these were then incubated with carboxyfluorescein succinimidyl ester (CFSE) stained THP-1 cells (5×10^4 cells per well) for 1 hour and washed with 15mM EDTA/PBS followed by PBS. Cells were then stained for biotin using Streptavidin-PE and read on a FACSAria II. Trogocytosis score was determined as the proportion of CFSE positive THP-1 cells also positive for streptavidin-PE less the no antibody control with waves run head-to-head.

Dimeric Fc gamma receptor binding ELISAs

High-binding 96 well ELISA plates were coated with 1 ug/mL spike protein in PBS overnight at 4 °C. Three wells on each plate were directly coated with 5 ug/mL IgG, isolated from healthy donors, and signals from these wells were used to normalize the Fc receptor activity of the plasma samples. Plates were washed with PBS and blocked with PBS/1 mM EDTA/1% BSA for 1 hour at 37°C. Plates were then washed and incubated with 1:10 diluted plasma for 1 hour at 37 °C and then with 0.2 ug/mL or 0.1 ug/mL of biotinylated FcγRIIa or FcγRIIIa dimer respectively (constructs kindly provided by Prof. Mark Hogarth from the Burnet Institute, Australia) for 1 hour at 37 °C.[36] Subsequently, a 1:10,000 dilution of Pierce high-sensitivity streptavidin-horseradish peroxidase (Thermo Scientific) was added for a final incubation for 1 hour at 37 °C. Lastly, TMB substrate (Sigma-Aldrich) was added, and color development was stopped with 1 M H_2SO_4 and absorbance read at 450 nm.

Quantification and statistical analysis

Analyses were performed in Prism (v9; GraphPad Software Inc, San Diego, CA, USA). Non-parametric tests were used for all comparisons. The Mann-Whitney and Wilcoxon tests were used for unmatched and paired samples, respectively. The Friedman test with Dunns correction for multiple comparisons was used for matched comparisons across variants. All correlations reported are non-parametric Spearman's correlations. p values less than 0.05 were considered to be statistically significant.